Tellus (2007), 59B, 251–259
Printed in Singapore. All rights reserved

TELLUS

Tropospheric methane in northern Finland: seasonal variations, transport patterns and correlations with other trace gases

By TUULA AALTO*, JUHA HATAKKA and MARKO LALLO, *Finnish Meteorological Institute, P.O. Box 503, FI-00101 Helsinki, Finland*

(Manuscript received 10 August 2006; in final form 8 January 2007)

ABSTRACT

Methane mixing ratios have been continuously observed at Pallas, Finland since winter 2004. The seasonal variation in monthly means was *ca.* 40 ppb, showing largest mixing ratios in winter and also high values during late summer. Examination of back-trajectories showed that the air masses with elevated methane mixing ratios arrived from continental Eastern and Central Europe while low methane mixing ratios were connected with Atlantic and Arctic air masses. During summer, air masses with highest mixing ratios arrived from Northwestern Russia indicating wetland sources, while the influence of southern emissions became more significant in winter. Methane was positively correlated with carbon dioxide and negatively correlated with ozone in winter. The average slope of the selected wintertime background hourly mean mixing ratios was 7.0 ± 1.2 ppb(CH_4)/ppm(CO_2). Nocturnal summertime low-altitude measurements above a local wetland source indicated slopes of about 10 ± 1 ppb(CH_4)/ppm(CO_2). The different slopes reflect the differences in emission parameters.

1. Introduction

The airborne mixing ratios of methane are influenced by atmospheric chemistry, natural surface sources and emissions due to human activity. In Northern Scandinavia and Russia, the natural surface sources are considered to be dominated by wetland emissions which have a strong seasonal cycle (e.g. Panikov and Dedysh, 2000; Heikkinen et al., 2002; Christensen et al., 2003; Friborg et al., 2003; Laurila et al., 2005). Anthropogenic methane sources, such as waste management, agriculture, biomass burning and fuel combustion also play a significant role and, as methane is relatively long-lived species, even Eastern and Central European sources (Levin et al., 1999; Biraud et al., 2000; Necki et al., 2003) may add to the observed tropospheric mixing ratio signal in the northern regions. The measurements at the Pallas Global Atmosphere Watch site in Northern Finland are considered in the current study. These observations near the northern limit of the Scandinavian boreal zone, some hundreds of kilometers east from Atlantic Ocean and west from Siberian gas fields, may show methane signals of very variable origin depending on the air mass flow patterns (see Jagovkina et al., 2000; Sidorov et al., 2002; Pedersen et al., 2005).

*Corresponding author.
e-mail: tuula.aalto@fmi.fi
DOI: 10.1111/j.1600-0889.2007.00248.x

The extent of Finnish wetland methane emissions has been the subject of much recent interest. Experimental chamber results from individual sites (e.g. Nykänen et al., 1998; Huttunen et al., 2003) have been utilized in upscaling to country-level by Minkkinen et al. (2002). The results are consistent with a recent inversion study using atmospheric methane observations (Bergamaschi et al., 2005), though it is shown that regional estimations derived from global inventories may produce variable results due to model and wetland distribution used. To add to the complexity of the issue, climatic warming with changing air and soil temperature and moisture is likely to affect the northern wetland methane emissions (e.g. Gorham, 1991; Hargreaves et al., 2001; Whiting and Chanton, 2001; Christensen et al., 2003). The possibility of future large methane emissions from Arctic marine geological reservoirs should also be noticed (Nisbet, 2002).

In recent years, the rise of methane mixing ratios in the atmosphere, previously very strong, has ceased (Dlugokencky et al., 2003). The causes of the marked change in the behaviour of methane are controversial. The interannual variability in growth rates has been attributed to several contributors involving changes in meteorology, chemical balance of the atmosphere and anthropogenic and natural emissions (e.g. Dlugokencky et al., 1998; Walter et al., 2001; Warwick et al., 2002; van der Werf, 2004). The presence of such multiple factors and causes emphasize the importance of continuously monitoring methane

mixing ratios within the region of vulnerable Northern ecosystems and changing emission trends.

Two years of continuous methane observations at Pallas are examined in this study. Seasonal mixing ratio variations and their connections to air mass flow patterns are studied using back-trajectories. Methane results are combined with simultaneous observations of carbon dioxide, ozone, nitrogen oxides and radon. The effect of local wetland emission dynamics is discussed.

2. Materials and methods

2.1. Site

Pallas site is located in the Pallas-Yllästunturi National Park in Northern Finland. The region is sparsely populated and relatively unpolluted, the nearest population centre of 2500 inhabitants is located at 19 km distance. There is no significant industrial activity in the region. The main station, Sammaltunturi, is located on the treeless top of an arctic hill (67°58′24″N, 24°06′58″E, 565 m a.s.l.). The terrain around the site is characterized by patches of boreal forests, wetlands and lakes. The nearest 20 km^2 consists of 6% open wetland. On the average, undrained, drained and forested mires comprize nearly one- third of Finland's land area, but due to the sloping characteristics of the Pallas region wetlands are in minority in the immediate vicinity of the station. Large-scale flat topography and wetlands extend east and south from Pallas towards Western Siberia. The coldest winter temperatures may drop below –30°C while warmest summer temperatures rise above 20°C. The ground is covered with snow usually from October to May. In December–January, there is a period when the sun is continuously below horizon, due to the location above the Arctic circle. Summer insolation is correspondingly high, with a period of 24-hr daylight in June/July.

2.2. Measurements

Several species relevant for atmospheric research are continuously monitored at the station. CH_4 mixing ratios are measured four times an hour with an automated gas chromatographic system (Agilent 6890N) equipped with a flame ionization detector for CH_4 detection. The measurement precision is 1.5 ppb. Calibration of the observed signal is made with a working standard by measuring it after every ambient air sample. The working standard is calibrated against NOAA/ESRL standard reference gases (NOAA04 standard scale) four to six times in a year. NOAA/ESRL/CCGG cooperative air sampling network flasks have also been collected at the station since 2002. The difference between continuous measurements and flask results was in average less than 1.5 ppb, analyzed from ambient air samples taken at close time intervals. The quality of the measurements was also verified by the recent intercomparison in the MethMonitEUr-project showing good agreement with other methane measurements made in the European network (Nisbet et al., 2005). CO_2 is measured with infrared gas analyzer (LI-6252) and calibrated using a system of working standards and NOAA/ESRL standards (Hatakka et al., 2003). O_3 and NO_x are monitored using instruments based on measuring UV absorbance (TEI 49 C) and chemiluminescence (TEI 42 CTL), which are calibrated four times a year. Airborne radon-222 (^{222}Rn) is measured with an instrument that is based on measuring the beta activity of aerosol collected continuously onto a filter (Hatakka et al., 2003). At a wetland (sedge fen) site Lompolojänkkä (67°59′50″N, 24°12′33″E, 269 m.a.s.l.) about 6 km distance from the hill site CH_4 and CO_2 are measured with another gas chromatograph system (Agilent 6890N) 20 times every hour from 2.8 and 1.4 m heights above the ground, 10 times each height. The wetland site results are also calibrated with standards from NOAA/ESRL, but because the system is constructed differently (one column system, shorter measurement time), the precision achieved does not quite reach that of Sammaltunturi.

2.3. Data selection and processing

In order to differentiate between local and regional signals, the hours with low wind speed and high mixing ratio variation were excluded from the methane data set. Based on wind statistics, during June–August the limit was 3 m s^{-1} and during rest of the year 4 m s^{-1}. The limit for the mixing ratio variation was 8 ppb in an hour for the whole year. Variation was used instead of hourly standard deviation, because there were only four measurements per hour. Together these limitations exclude 27% of the data. Similar rules were applied to other mixing ratio data (hourly standard deviation limits for CO_2 were 0.5 ppm for July–August and 0.3 ppm otherwise). Data collected in poorly mixed conditions are also important for studying local issues. Unselected data were used in connection with measurements at local wetland.

Methane mixing ratios were compared to other species, assessing simultaneous mixing ratio variation due to changes in transport which occur in time span of few hours to weeks. Mixing ratios of species like CO_2 increase from year to year and have strong annual cycles, and thus the variations which occur in monthly or longer timescales were removed from the data before comparison. For this purpose, a function consisting of a third order polynomial for the growth rate and four harmonic terms for the annual cycle was fitted to the data and the residuals were filtered according to the widely used methods by Thoning et al. (1989). The filtering removed variations with periods less than 2 months. The filtered results were added to the function, which was again subtracted from the original data leaving residuals that contained the high-frequency variation (see Harris et al. (2000) for similar treatment of Barrow results). This procedure was performed for methane, carbon dioxide and ozone data, and the residuals were intercompared. Slopes of methane versus carbon dioxide were calculated using geometric mean regression.

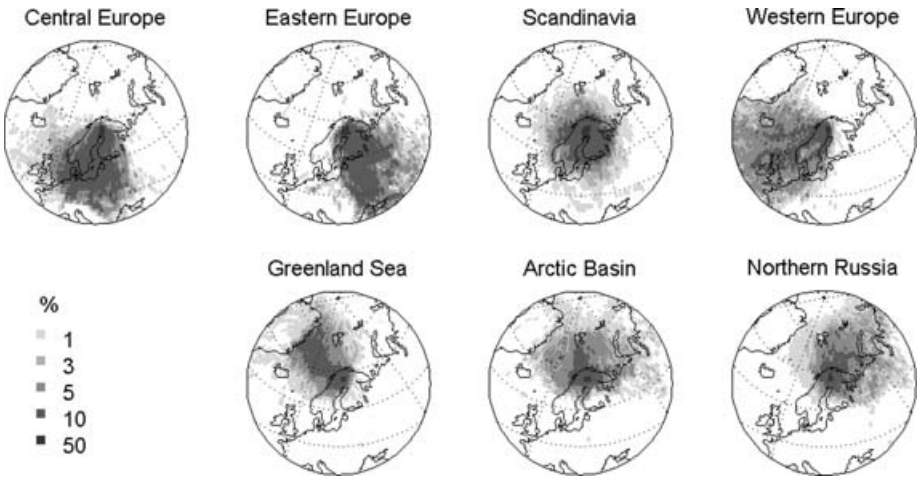

Fig. 1. Clusters of air mass transport trajectories arriving at Pallas during 2004–2005. The different grey shadings refer to number of crossings in the $1^\circ \times 1^\circ$ grid squares, expressed as percentage of the total number of trajectories.

2.4. Trajectories

Trajectories, i.e. paths of air parcels arriving at Pallas, were utilized in analysis of long-range transport of methane. They were calculated five days backwards using a three- dimensional kinematic FLEXTRA trajectory model (e.g. Stohl et al., 1995; Stohl and Seibert, 1998), using numerical meteorological data from the European Centre for Medium-Range Weather Forecasts (ECWMF) MARS database. Trajectories were calculated once in every three hr and their arrival level at Pallas was 925 hPa.

The trajectories were clustered according to the method by Eneroth et al. (2005). In the clustering method (hereafter CM), trajectories are arranged to groups according to their distances, i.e. trajectories with similar air parcel transport paths are assigned into the same group. The optimal number of groups is determined by the cost of combining different groups together. The climatological analysis by Eneroth et al. (2005) was made for 1998–2003. In this work, the CM method was applied for years 2004 and 2005. Similar results were obtained for this later period yielding seven groups of trajectories describing the different transport patterns to Pallas (Fig. 1). The groups are named here as Central Europe, Western Europe, Eastern Europe, Scandinavia, Greenland Sea, Arctic Basin and Northern Russia cluster, respectively. Compared to earlier work, Eastern Europe cluster corresponds to West Russia cluster, Scandinavia to Norwegian Sea cluster and Greenland Sea to Atlantic cluster. Names were changed to describe better the small changes in cluster orientation. Methane observations were further assigned into different clusters according to the corresponding trajectory arrivals.

Trajectories were also applied to constructing maps of methane source regions, as was done in earlier work by Aalto et al. (2002). In this method (hereafter SM), the mixing ratio observations are distributed along the corresponding trajectory paths (Stohl, 1996). In the first step, the mixing ratios are distributed evenly along the path and averaged at every grid point crossed by several paths and thus multiple mixing ratio values. Mixing ratios are scaled and redistributed again along the trajectory path by following methods developed by Stohl (1996). Redistribution continues until the change in resulting mixing ratio field is negligible. Finally, a chart is obtained where high mixing ratio regions refer to multiple occasions of air masses with elevated mixing ratios passing that region before arriving at Pallas. Trajectory altitudes $<$1000 m were included in order to allow only transport inside the boundary layer and continuous contact with the surface sources.

3. Results

3.1. Annual variation

Methane observed at Pallas showed a somewhat indistinct annual cycle with highest mixing ratios occurring in the course of winter (Fig. 2). A period of large mixing ratio variation and highly elevated maximum values was noticeable during late summer. The yearly range in monthly means was *ca.* 40 ppb, with highest values occurring in November–March and lowest during June and early July (Table 1). The mixing ratios started to rise again in July when temperatures prevailed above 10°C for several days and there were air flows coming from continental (eastern) directions. The mixing ratios also showed some daily variation with build-up of methane during calm, warm nights and release after sunrise. The mean diurnal variation in well-mixed air masses was $<$10 ppb in July and according to unselected data about 17 ppb. During winter months, the diurnal variation was almost non-existent for methane, as well as for CO_2, O_3 and ^{222}Rn. According to preliminary analysis of the flux measurements made in 2005 in a nearby sedge fen (Lompolojänkkä fen), the methane emissions started in June, reached their maximum level in early July and started to decrease in August. The local wetland emissions may influence the observed mixing ratios, but

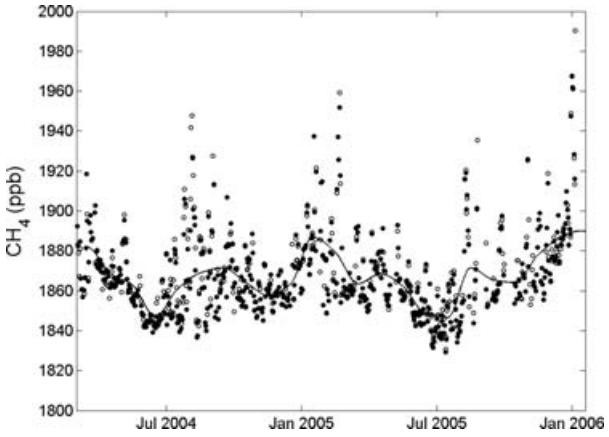

Fig. 2. Methane mixing ratios observed at Pallas during 2004–2005. Filled circles are daily means obtained from selected background data, and open circles refer to unselected data. The line represents smoothed monthly means according to selected data.

Table 1. Monthly mean mixing ratios of selected background methane observations at Pallas

Month	Year 2004 CH_4 (ppb)	Year 2005 CH_4 (ppb)
1	-	1886
2	1878	1878
3	1882	1862
4	1869	1869
5	1863	1861
6	1847	1848
7	1859	1846
8	1866	1868
9	1870	1864
10	1864	1865
11	1857	1877
12	1862	1887

the influence is mainly confined to weak mixing conditions, since high mixing ratio episodes were observed also during times out of the active local emission period showing long-range transport of signals of similar magnitude. Also, during times, when local emissions were large, there were days when very low and stable methane mixing ratio levels were observed. The summer high mixing ratio episodes started a few weeks later in 2005 than in 2004, which was reflected in the low monthly mean for July 2005 (Table 1). The monthly means were similar to the maritime reference level (Globalview-CH_4, 2005) during April–June 2004, but the July–September means were higher by about 20 ppb. The mixing ratio decreased and the variation suppressed again in September or October in anticipation of substantial transport events in November and December lasting for several hours or days.

3.2. Trajectory studies

Methane observations were combined to corresponding trajectory arrivals, which were assigned to different transport clusters by the CM method. Averaged well-mixed mixing ratio values for each cluster are shown in Table 2. Means were calculated for all data and for winter and summer separately. Eastern Europe cluster showed the highest means for both winter and summer. There were fewer trajectories belonging to this cluster during spring and early summer. The second highest mean mixing ratios appeared in the Central Europe cluster, and were also less frequent during spring and early summer. The third highest mixing ratios were found in Scandinavia and Northern Russia clusters. The Scandinavia cluster was very large in number, consisting of relatively curved and short trajectories circling in Fennoscandia and neighboring regions in Northwestern Russia and Norwegian Sea. The Northern Russia cluster consisted partly of long trajectories stretching over the Barents Sea but also included trajectories crossing the large wetland and gas manufacturing areas in Ob river region. In July 2005, there were no trajectories in the Eastern Europe, Central Europe or Northern Russia clusters, explaining the low July mean for that year. Arctic Basin, Greenland Sea and Western Europe clusters with more marine characteristics showed the lowest mixing ratios, in agreement with earlier results for CO_2 (Eneroth et al., 2005).

Possible methane emission areas influencing observations at Pallas were assessed by the SM method. A mixing ratio chart was created for winter (October–April) and summer (July–September) separately (Fig. 3). This rough division was used, because the SM method is not well suited to examinations of very short time periods due to small amount of trajectory material suppressing the resulting chart area to impractically small size. During summer, the high mixing ratios were transported from Northwestern Russia, possibly indicating wetland emissions. It is also possible that transport from further east is reflected in the results, making it more difficult to identify the exact emission areas. During winter, the southern emissions become more visible probably because the snow cover, and low temperature reduce natural emissions in the northern regions. The winter results agree qualitatively with gridded Edgar emission database (Olivier et al., 2005) for anthropogenic emissions including mid- and northern latitude sources, such as landfills, sewage, ruminants, coal mining and natural gas production (Siberian gas fields) and fuel usage. In comparison to the CM method, the Eastern Europe cluster (Fig. 1) covers best the summer and winter high mixing ratio regions shown in the charts. In accordance, the mean mixing ratios were highest in this cluster (Table 2). The Scandinavian and Northern Russian clusters also contribute to some extent to the summer emission regions and the Central European cluster to the winter emission regions indicated by SM method. The difference between summer and winter emissions is supported by the results for cluster mean mixing ratios, since the summer mean for the Central Europe cluster is somewhat low when compared

Table 2. Average methane mixing ratios in each transport cluster, selected for winter months (November–March) and summer months (July–September). Also shown are winter slopes of methane versus carbon dioxide mixing ratio and their correlation coefficients (r). F refers to the frequency of the cluster, i.e. number of trajectories in the cluster divided by number of all trajectories

Cluster	F (%)	Mean CH_4 (ppb)	Summer CH_4 (ppb)	Winter CH_4 (ppb)	Winter slope $\frac{ppb(CH_4)}{ppm(CO_2)}$	r
Central Europe	10	1876	1868	1886	7.8 ± 1.1	0.88
Eastern Europe	6	1897	1905	1901	8.1 ± 1.2	0.83
Scandinavia	27	1870	1864	1883	7.1 ± 1.2	0.86
Western Europe	14	1859	1857	1861	6.0 ± 1.4	0.72
Greenland Sea	11	1856	1852	1861	5.2 ± 1.5	0.68
Arctic Basin	13	1858	1845	1862	7.3 ± 1.4	0.74
Northern Russia	19	1870	1871	1879	6.7 ± 1.2	0.87

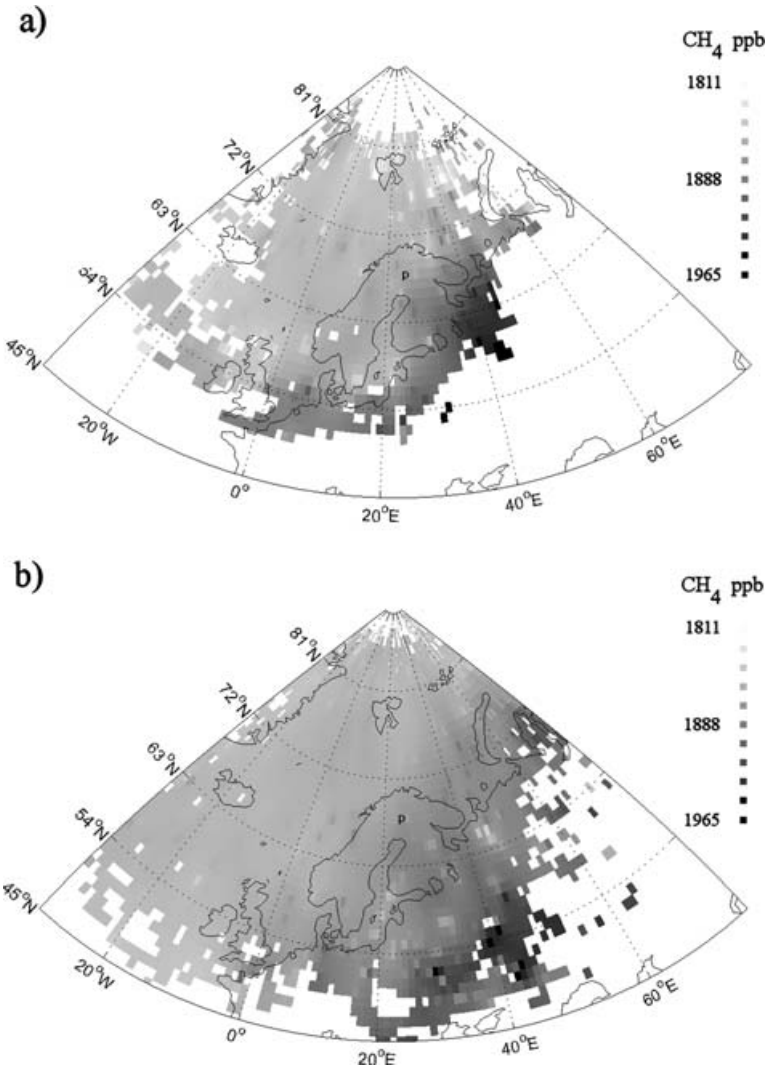

Fig. 3. Methane mixing ratio distributions for air masses arriving at Pallas (p) during (a) summer (July–September) and (b) winter (October–April).

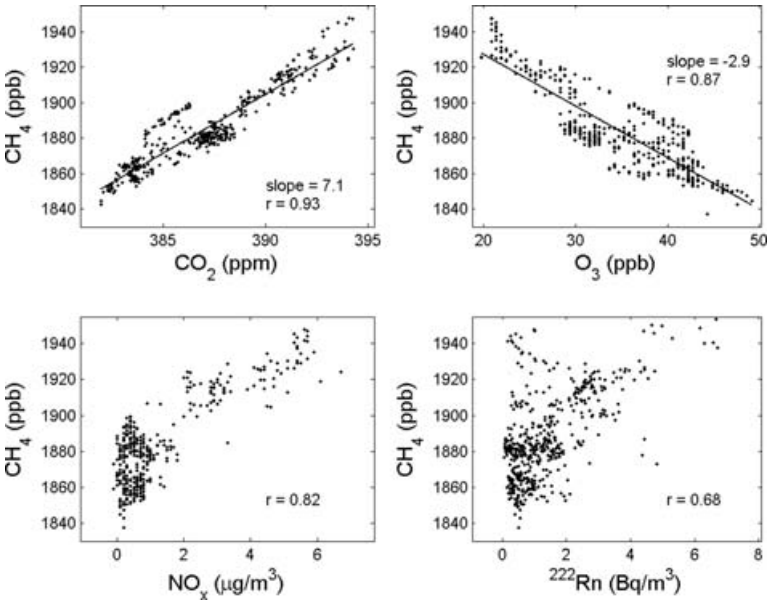

Fig. 4. Methane versus carbon dioxide, ozone, nitrogen oxide and radon mixing ratios at Pallas during January 2005.

to winter mean. According to both methods, air masses with elevated methane mixing ratios are only rarely transported from marine regions.

3.3. Correlations with other species

Methane had common features with carbon dioxide observed at Pallas. The correlation was strongly positive in winter and weak in summer, turning often to anticorrelation due to daytime photosynthetical uptake of carbon dioxide. Correlations for January 2005 are shown in Fig. 4. Observations were further filtered and the growth trend and annual cycles were removed using methods explained in Subsection 2.3, in order to focus on variations caused by changes in transport which occur in shorter than monthly timescales (see also Harris et al., 2000). Correlations for winter observations treated this way are shown in Fig. 5 with a slope of 7.0 ± 1.2 ppb(CH_4)/ppm(CO_2), showing results similar to those for unmodified observations.

The different clusters showed some deviation in their CH_4/CO_2 slopes (Table 2). The highest slopes of about of 8 ppb(CH_4)/ppm(CO_2) appeared in the Eastern Europe and Central Europe clusters, while the slope in the Greenland Sea cluster was only 5.2 ± 1.5 ppb(CH_4)/ppm(CO_2) (Fig. 5). Correlation between CO_2 and CH_4 was relatively high in all clusters. Slopes were also calculated separately for individual episodes, since during winter, the mixing ratios at Pallas are usually rather stable for days and then increase remarkably within couple of hours due to synoptic scale changes in air mass transport. These individual slopes showed, in average, results very similar to clustered observations. However, the variation was large and some single events indicated very high slopes of over 20 ppb(CH_4)/ppm(CO_2). The highest slopes were observed in connection with air mass transport from Eastern Europe, Central Europe and most interestingly

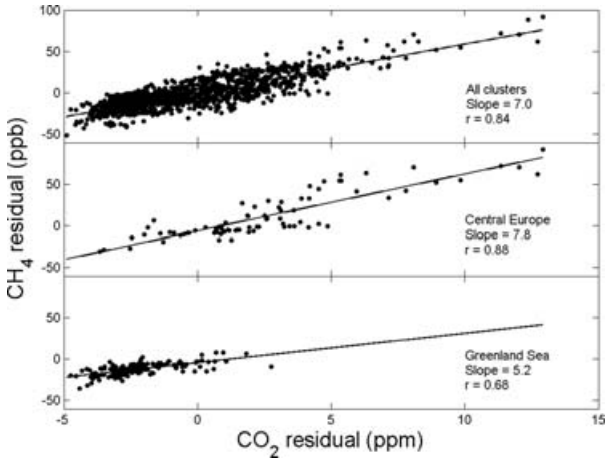

Fig. 5. Methane versus carbon dioxide residuals for different air mass transport clusters, calculated using November–March observations at Pallas.

from Northern Siberia Ob region (Fig. 6). Large methane emissions, relative to those of carbon dioxide, may indicate contributions from certain industrial or other anthropogenic processes as well as natural wetland sources, though our local wetland results did not show exceptionally high slopes.

The measurements at the local wetland site Lompolojänkkä included both methane and carbon dioxide mixing ratio observations at 1.4 m and 2.8 m height. The mixing ratios were significantly higher than at the Sammaltunturi hill site. Especially, on calm summer nights, the accumulated methane mixing ratios at the wetland site may reach values that are hundreds of ppbs higher than the hill site values. The CH_4/CO_2 slopes were steeper closer to ground (Fig. 7), but the values were not very different from clustered long-range transport results. The

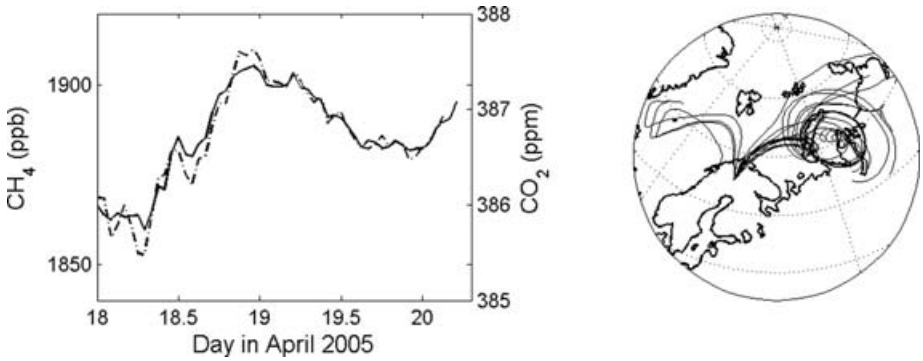

Fig. 6. Methane (solid line) and carbon dioxide (dash-dot line) mixing ratios in 18–20 April 2005 and corresponding trajectories stretching five days backwards. The low mixing ratios during 18 April were observed in connection with air mass transport from west (Greenland Sea), while the subsequent increase coincided with transport from Ob river region. The slope of this episode was 22 ± 1 ppb(CH_4)/ppm(CO_2).

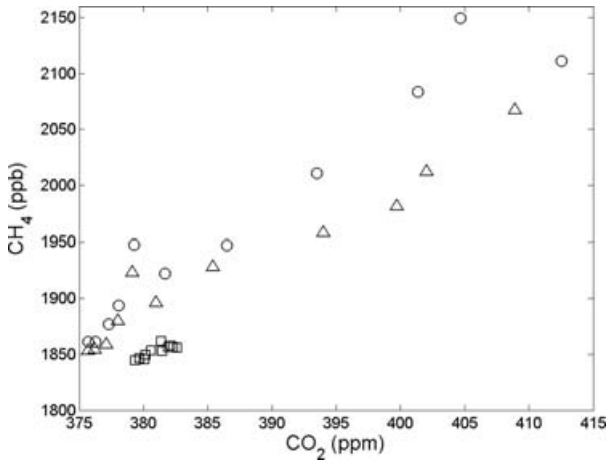

Fig. 7. Methane mixing ratios at the wetland site (circles: 1.4 m above ground, triangles: 2.8 m above ground) and at the hill site (squares) from 20:00 to 06:00 local time in 14–15 June 2005. The altitude difference between the wetland site and the hill site is about 300 m.

average for individual summer night mixing ratio increases at 1.4 m height was about 10.8 ± 1.1 ppb(CH_4)/ppm(CO_2) and at 2.5 m about 9.0 ± 1.1 ppb(CH_4)/ppm(CO_2) (unselected data).

Methane was negatively correlated with ozone during winter (Fig. 4). Correlations of carbon dioxide with ozone were even higher with $r = 0.95$, indicating a possibility to use the slope as a starting point for determining anthropogenic NO_x/CO_2 emission ratios (Harris et al., 2000). Significant differences in CO_2/O_3 slopes were not found between clusters. The mixing ratio of NO_x was usually near observation limit at Pallas and thus, the correlation was not very clear. However, when the longer-lived NO_2 showed increase, methane and carbon dioxide levels were often also elevated. Methane was not very strongly correlated with radon (Fig. 4), possibly due to the snow pack and complex soil structure creating a weak and spatially variable emission pattern, while high methane was probably of long-range transported anthropogenic origin. Transport from marine and continental regions did not show significant differences. During some (summer half year) mornings, a peak in radon mixing ratios was observed due to the release of the lower-level inversion, bringing air masses with nocturnally accumulated higher radon mixing ratio to the station altitude. However, methane and carbon dioxide mixing ratios only rarely showed increase at the same time indicating only limited influence of the local sources.

4. Discussion

Methane mixing ratios observed at Pallas in wintertime generally increased simultaneously with other anthropogenically produced and long-range transported species, like carbon dioxide and nitrogen oxides. During these episodes, the trajectories typically showed air mass transport from continental southern and eastern directions. During the snow-free season the mixing ratio variations of methane and other species diverged to some extent due to increased variety in natural surface sources and sinks and changes in air chemistry. The onset of wetland methane emissions in northern regions along with springtime temperature rise, soil thaw and ground vegetation growth was reflected in the observed methane mixing ratios.

The methane levels showed similarities to the maritime reference level (Globalview-CH_4, 2005) most often during April, May and June, while otherwise the values were usually higher. The annual cycle was not very clear, as noted also for some Central European continental background sites (Schmidt et al., 1996; Necki et al., 2003). The summer maximum was also observed at Fraserdale by Worthy et al. (2000), due to Canadian wetland emissions and corresponding high mixing ratios transported to the site. However, when transport from Atlantic and Arctic to Pallas was considered, the late summer increase nearly disappeared creating a longer and more distinct summer minimum. Such annual variation can be mainly created by large-scale transport and changes in air chemistry where seasonality of OH radical evokes a seasonal cycle in methane mixing ratios (see e.g. Cunnold et al., 2002).

Trajectory studies by CM and SM methods were in good agreement indicating emissions from continental Central and

Eastern Europe. The winter results agreed qualitatively with the anthropogenic CH_4 emission database (Olivier et al., 2005). It can be concluded that both CM and SM are useful in explaining the characteristics of methane observed at Pallas, though their applications may be somewhat different depending on the timescales investigated, favouring CM for short time periods, and SM for the need to recognize spatially well defined source regions. It is possible that some of the summer events were caused by biomass burning (Kasischke and Bruhwiler, 2003; van der Werf et al., 2004), but they are difficult to extract from the current data due to small number of suitable episodes and multiplicity of other possible sources.

The winter slopes of CH_4 and CO_2 were rather similar to Schauinsland, Germany (7.8 ppb(CH_4) /ppm(CO_2) for half hourly means, 6.5 ppb(CH_4) /ppm(CO_2) for monthly means, Schmidt et al., 1996) and lower in comparison to Syktyvkar, Russia (11.6, Sidorov et al., 2002), Kasprowy Wierch, Poland (9.5–12, Necki et al., 2003) and Barrow, Alaska (12.8) and Alert, Canada (9–16), for slopes determined for Siberian transport trajectories (Worthy et al., 1994; Harris et al., 2000). Some studies indicate even higher slopes for Alert (Conway and Steele, 1989). Our results for a local sedge fen indicated slopes similar or slightly higher than long-range transported wintertime anthropogenic emissions. The differences to other studies may be partly due to different methodology and treatment of results, but there are probably also other factors contributing, whether related to changes in anthropogenic emissions (see Dlugokencky et al., 2003) or dominance of natural emissions. Methane and carbon dioxide isotopes would be a helpful tool in studying the origins of the emissions and resulting slopes.

The methane observations at Pallas showed variable signals depending on the prevailing transport patterns. Vast Northern wetlands in the surrounding boreal zone extending east over Siberia and anthropogenic emissions at mid- and northern latitudes together created a seasonally varying continental methane source including both local and long-range transported components observed at Pallas. On the other hand, the majority of observed air masses were transported over marine Atlantic and Arctic Basins bringing low background mixing ratios. The interplay of changes in meteorology and emissions provides good arguments to continue monitoring the long-term trends in methane mixing ratios at Pallas. In the future, it would also be useful to deepen the multi-component analysis and expand it to species like CO, N_2O and H_2.

5. Acknowledgements

We would like to thank Kristina Eneroth for introducing us to trajectory clustering. The cooperation with the Finnish Forest Research Institute, Pallas-Yllästunturi National Park, and financial support from MethMonitEUr project (European Commission, contract EVK2-CT-2002-00175) and the Nessling foundation are gratefully acknowledged.

References

Aalto, T., Hatakka, J., Paatero, J., Tuovinen, J.-P., Aurela, M. and co-authors. 2002. Tropospheric carbon dioxide concentrations at a northern boreal site in Finland: basic variations and source areas. *Tellus* **54B**, 110–126.

Bergamaschi, P., Krol, M., Dentener, F., Vermeulen, A., Meinhardt, F. and co-authors. 2005. Inverse modeling of national and European CH_4 emissions using the atmospheric zoom model TM5. *Atmospheric Chemistry and Physics* **5**, 2431–2460.

Biraud, S., Ciais, P., Ramonet, M., Simmonds, P., Kazan, V. and co-authors. 2000. European greenhouse gas emissions estimated from continuous atmospheric measurements and radon 222 at Mace Head, Ireland. *J. Geophys. Res.* **105**(D1), 1351–1366.

Christensen, T. R., Ekberg, A., Ström, L., Mastepanov, M., Panikov, N. and co-authors. 2003. Factors controlling large scale variations in methane emissions from wetlands. *Geophys. Res. Lett.* **30**(7), 1414, doi: 10.1029/2002GL016848.

Conway, T. J. and Steele, L. P. 1989. Carbon dioxide and methane in the Arctic atmosphere. *J. Atmos. Chem.* **9**, 81–99.

Cunnold, D. M., Steele, L. P., Fraser, P. J., Simmonds, P. G., Prinn, R. G. and co-authors. 2002. In situ measurements of atmospheric methane at GAGE/AGAGE sites during 1985-2000 and resulting source inferences. *J. Geophys. Res.* **107**(D14), 4225, doi: 10.1029/2001JD001226.

Dlugokencky, E. J., Masarie, K. A., Lang, P. M. and Tans, P. P. 1998. Continuing decline in the growth rate of the atmospheric methane burden. *Nature* **393**, 447–450.

Dlugokencky, E. J., Houweling, S., Bruhwiler, L., Masarie, K. A., Lang, P. M. and co-authors. 2003. Atmospheric methane levels off: Temporary pause or a new steady-state? *Geophys. Res. Lett.* **30**(19), 1992, doi: 10.1029/2003GL018126.

Eneroth, K., Aalto, T., Hatakka, J., Holmén, K., Laurila, T. and co-authors. 2005. Atmospheric transport of carbon dioxide to a baseline monitoring station in northern Finland. *Tellus* **57B**, 366–374.

Friborg, T., Soegaard, H., Christensen, T. R., Lloyd, C. R. and Panikov, N. S. 2003. Siberian wetlands: Where a sink is a source. *Geophys. Res. Lett.* **30**(21), 2129, doi: 10.1029/2003GL017797.

GLOBALVIEW-CH4: Cooperative Atmospheric Data Integration Project - Methane. CD-ROM, NOAA/CMDL, Boulder, Colorado. [Also available on Internet via anonymous FTP to ftp.cmdl.noaa.gov, Path: ccg/ch4/GLOBALVIEW], 2005.

Gorham, E. 1991. Northern peatlands: Role in the carbon cycle and probable responses to climatic warming. *Ecological Applications* **1**, 182–195.

Hatakka, J., Aalto, T., Aaltonen, V., Aurela, M., Hakola, H. and co-authors. 2003. Overview of atmospheric research activities and results at Pallas GAW station. *Boreal Environment Research* **8**, 365–384.

Hargreaves, K. J., Fowler, D., Pitcairn, C. E. R. and Aurela, M. 2001. Annual methane emission from Finnish mires estimated from eddy covariance campaign measurements. *Theor. Appl. Climatol.* **70**, 203–213, doi:10.1007/s007040170015.

Harris, J. M., Dlugokencky, E. J., Oltmans, S. J., Tans, P. P., Conway, T. J. and co-authors. 2000. An interpretation of trace gas correlations during Barrow, Alaska, winter dark periods, 1986–1997. *J. Geophys. Res.* **105**(D13), 17267–17278.

Heikkinen, J. E. P., Elsakov, V. and Martikainen, P. J. 2002. Carbon dioxide and methane dynamics and annual carbon balance in tundra wetland in NE Europe, Russia. *Global Biogeochemical Cycles* **16**(14), 115, doi: 10.1029/2002GB001930.

Huttunen, J. T., Nykänen, H., Turunen, J. and Martikainen, P. J. 2003. Methane emissions from natural peatlands in the northern boreal zone in Finland, Fennoscandia. *Atmos. Environ.* **37**, 147–151.

Jagovkina, S. V., Karol, I. L., Zubov, V. A., Lagun, V. E., Reshetnikov, A. I. and co-authors. 2000. Reconstruction of the methane fluxes from the west Siberia gas fields by the 3D regional chemical transport model. *Atmos. Environ.* **34**, 5319–5328.

Kasischke, E. S. and Bruhwiler, L. P. 2003. Emissions of carbon dioxide, carbon monoxide, and methane from boreal forest fires in 1998. *J. Geophys. Res.* **108**(D1), 8146, doi: 10.1029/2001JD000461.

Laurila, T., Aurela, M., Lohila, A. and Tuovinen, J.-P. 2005. Trace gas and CO_2 contributions of northern peatlands to global warming potential. In: *The Carbon Balance of Forest Biomes* (eds H. Griffiths and P. G. Jarvis), Taylor & Francis, Oxford, UK, 270–292.

Levin, I., Glatzel-Mattheier, H., Marik, T., Cuntz, M. and Schmidt, M. 1999. Verification of German methane emission inventories and their recent changes based on atmospheric observations. *J. Geophys. Res.* **104**(D3), 3447–3456.

Minkkinen, K., Korhonen, R., Savolainen, I. and Laine, J. 2002. Carbon balance and radiative forcing of Finnish peatlands 1900-2100 - the impact of forestry drainage. *Global Change Biol.* **8**, 785–799.

Necki, J., Schmidt, M., Rozanski, K., Zimnoch, M., Korus, A. and co-authors. 2003. Six-year record of atmospheric carbon dioxide and methane at a high-altitude mountain site in Poland. *Tellus* **55B**, 94–104.

Nisbet, E. 2002. Have sudden large releases of methane from geological reservoirs occurred since the Last Glacial Maximum, and could such releases occur again? *Phil. Trans. R. Soc. Lond.* **A360**, 581–607.

Nisbet, E. (Ed.) and participant partners. 2005. Methane Monitoring in the European region (MethMonitEUr). Final Report in EC 5th Framework Programme "Environment and Sustainable Development", Reporting Period Feb 1, 2003 - Jan 31, 2005, Contract EVK2-CT-2002-00175. Available at http://www.gl.rhul.ac.uk/METH/MonitEUr/final/MethMonFinal.htm.

Nykänen, H., Alm, J., Silvola, J., Tolonen, K. and Martikainen, P. J. 1998. Methane fluxes on boreal wetlands of different fertility and the effect of long-term experimental lowering of the water table on flux rates. *Global Biogeochem. Cycles* **12**(1), 53–69.

Olivier, J. G. J., Van Aardenne, J. A., Dentener, F., Ganzeveld, L. and Peters, J. A. H. W. 2005. Recent trends in global greenhouse gas emissions: regional trends and spatial distribution of key sources. In: *Non-CO2 Greenhouse Gases (NCGG-4)* (ed A. van Amstel), Millpress, Rotterdam, 325–330.

Panikov, N. S. and Dedysh, S. N. 2000. Cold season CH_4 and CO_2 emission from boreal peat bogs (West Siberia): Winter fluxes and thaw activation dynamics. *Global Biogeochem. Cycles* **14**, 1071–1080.

Pedersen, I.-T., Holmén, K. and Hermansen, O. 2005. Atmospheric methane at Zeppelin Station in Ny-Ålesund: presentation and analysis of *in situ* measurements. *Journal of Environmental Monitoring* **7**(5), 488–492.

Schmidt, M., Graul, R., Sartorius, H. and Levin, I. 1996. Carbon dioxide and methane in continental Europe: a climatology, and ^{222}Radon-based emission estimates. *Tellus* **48B**, 457–473.

Sidorov, K., Sogachev, A., Langendörfer, U., Lloyd, J., Nepomniachii, I. L. and co-authors. 2002. Seasonal variability of greenhouse gases in the lower troposphere above the eastern European taiga (Syktyvkar, Russia). *Tellus* **54B**, 735–748.

Stohl, A., Wotawa, G., Seibert, P. and Kromp-Kolb, H. 1995. Interpolation errors in wind fields as a function of spatial and temporal resolution and their impact on different types of kinematic trajectories. *J. Appl. Meteorol.* **34**, 2149–2165.

Stohl, A. 1996. Trajectory statistics - A new method to establish source-receptor relationships of air pollutants and its application to the transport of particulate sulfate in Europe. *Atmos. Environ.* **30**, 579–587.

Stohl, A. and Seibert, P. 1998. Accuracy of trajectories as determined from the conservation of meteorological tracers. *Qtr. J. R. Meteor. Soc.* **124**, 1465–1484.

Walter, B. P., Heimann, M., Matthews, E. 2001. Modeling modern methane emissions from natural wetlands 2. Interannual variations 1982-1993. *J. Geophys. Res.* **106**(D24), 34 207–34 219.

van der Werf, G. R., Randerson, J. T., Collatz, G. J., Giglio, L., Kasibhatla, P. S. and co-authors. 2004. Continental-scale partitioning of fire emissions during the 1997 to 2001 El Niño/La Niña period. *Science* **303**, 73–76.

Thoning, K. W., Tans, P. P., Komhyr, W. D. 1989. Atmospheric carbon dioxide at Mauna Loa Observatory 2. Analysis of the NOAA GMCC data, 1974-1985. *J. Geophys. Res.* **94**, 8549–8565.

Warwick, N. J., Bekki, S., Law, K. S., Nisbet, E. G. and Pyle, J. A. 2002. The impact of meteorology on the interannual growth rate of atmospheric methane. *Geophys. Res. Lett.* **29**(20), 1944–1947.

Whiting, G. J. and Chanton, J. P. 2001. Greenhouse carbon balance of wetlands: methane emission versus carbon sequestration. *Tellus* **53B**, 521–528.

Worthy, D. E. J., Trivett, N. B. A., Hopper, J. F. and Bottenheim, J. W. 1994. Analysis of long-range transport events at Alert, Northwest Territories, during the Polar Sunrise Experiment. *J. Geophys. Res.* **99**(D12), 25329–25344.

Worthy, D. E. J., Levin, I., Hopper, F., Ernst, M. K. and Trivett, N.B. A. 2000. Evidence for a link between climate and northern wetland methane emissions. *J. Geophys. Res.* **105**(D3), 4031–4038.